Preliminary Study on the Duration of High-Frequency Seismic Waves in Northern Taiwan from Deep Regional Earthquakes

Haekal A. Haridhi[1,2,3,*], *Bor Shouh* Huang[4], *Muhammad* Faizi[2], *Putri* Ramadhan[2], *Ridrya A. A.* Harahap[2], *Nurhadi* Ismanto[2], *Dimas* Sianipar[5]

[1]Tsunami and Disaster Mitigation Research Center (TDMRC), Universitas Syiah Kuala, Banda Aceh 23111, Indonesia
[2]Research Center for Marine Sciences and Fisheries, Universitas Syiah Kuala, Banda Aceh 23111, Indonesia
[3]Department of Marine Sciences, Faculty of Marine and Fisheries, Universitas Syiah Kuala, Banda Aceh 23111, Indonesia
[4]Institute of Earth Science, Academia Sinica, Taipei 115, Taiwan
[5]Agency for Meteorology, Climatology, and Geophysics (BMKG), Jakarta 10610, Indonesia

Abstract. The high-frequency seismic waves are usually generated by shallow earthquakes and is observed at a location near the earthquake source. Seismic energy tends to attenuate as it propagates through the Earth's surface and interior; however, this is not the case at the subduction zone. A regional earthquake that occurred within the subducting slab was observed to have high-frequency energy, although it is from the deep (i.e. > 100 km) and with moderate magnitude (i.e. Mw 5). This phenomenon resulted from the slab effect on focusing the earthquake signal or known as the guided wave. Taiwan has a complicated tectonic feature, where Taipei city, its capital, sits above the oblique subduction of Philippine Sea Plate (PSP), i.e. the southern Ryukyu subduction zone, enhancing its exposure to strong shaking resulting from the deep regional earthquakes. In this study, we use six regional earthquakes at the southern Ryukyu subduction zone recorded by the Formosa Array (FM Array). The FM Array is a dense seismic network with a total of 140 stations located in the northern part of Taiwan, with the distance between stations approximately 5 kilometers. With high-resolution data, we could identify the distribution of the guided wave phenomenon through body wave dispersion of deep regional earthquake signals, where only stations above 10 – 20 km from the plate interface showed dispersion. An Hp/Lp ratio with a 5-second moving window is applied to the dispersed signal. The results indicate that the high-frequency signal has a longer duration at stations that sit 10 to 20 km above the plate interface. This study suggests that the slab effect will produce an anomalous seismic intensity at the subduction region and should be considered in the Ground Motion Prediction Equation (GMPE) so that the damaged to buildings resulting from strong shaking could be reduced.

1 Introduction

The guided wave phenomena generated by deep regional earthquakes have been reported in subduction zone around the world [1–9]. The seismogram that exhibit these guided characteristics are indicated by their high-frequency content, large amplitude with distortion of *P* and *S* wave pulses, and low-frequency arrivals preceding the high-frequency energy [1,3]. These characteristics have been explained through various findings, such as the existence of the low-velocity layer of the former oceanic crust at the top of the subducting plate [3,5,10], small-scale heterogeneity of velocity within the subducting plate [7], and the geometry of the subducting plate [4].

In addition to their seismogram characteristics, the guided waves in the subduction zone cause large intensity in the fore-arc area, even though they are not felt at their epicentre and the back-arc area [1,8,9]. In the fore-arc stations, where there's a significant concentration of high intensity, the broadband seismograms display amplitudes that are tens to several hundred times greater than those observed at a corresponding back-arc station within the frequency range of 4 to 20 Hz [1]. It is commonly known that high-frequency seismic waves, which resulted in large intensity, are typically observed in locations near the earthquake source or hypocentre. However, due to the guiding effect, the deep regional earthquake can induce large intensity despite their moderate magnitude and long distance [6,7]. Thus, it is important to study this guiding effect on its high-frequency and duration. Unlike shallow earthquakes, which have received extensive study, deep regional earthquakes and their characteristics have received comparatively less attention.

The lesson learned of the April 14, 1909 Taiwan earthquake particularly emphasize the importance of studying deep regional earthquakes. This event caused 9 deaths, 51 injuries, 122 houses were destroyed, 252 houses were partially destroyed and 798 houses were damaged [11]. Nowadays, with significantly increase in population, infrastructure, and the economy, it is even more important to study the potential damage that can be induced by the large intensity of deep earthquake at the Northern Taiwan, where its capital Taipei is located.

* Corresponding author: haekal.azief.haridhi@usk.ac.id

© The Authors, published by EDP Sciences. This is an open access article distributed under the terms of the Creative Commons Attribution License 4.0 (https://creativecommons.org/licenses/by/4.0/).

2 Seismotectonic Background

Taiwan is located between two convergent plate boundaries: one between the Eurasian Plate (EUP) and the Philippine Sea Plate (PSP) in southern Taiwan, where the EUP subducts beneath the PSP at the Manila Trench, and the other in northern Taiwan, where the PSP subducts beneath the EUP at the Ryukyu Trench [12] (Fig. 1a and b).

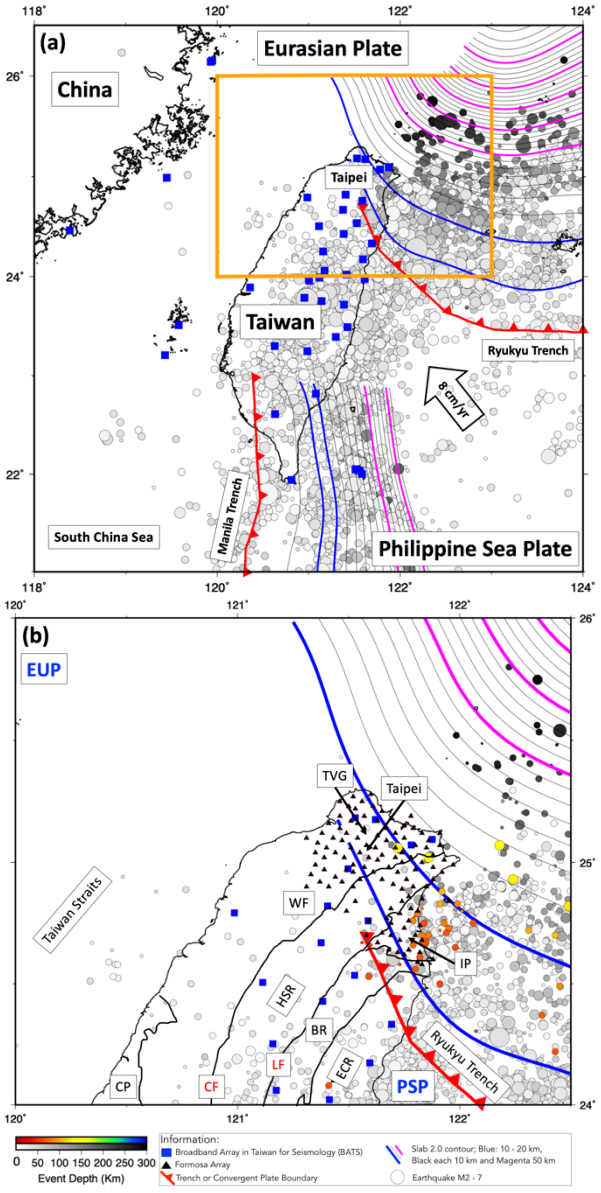

Fig. 1. (a) Taiwan is situated between two convergent plate boundaries. In northern Taiwan, the Philippine Sea Plate (PSP) obliquely subducts beneath the Eurasian Plate (EUP) at the Ryukyu Trench, with a motion of 8 cm/year. In southern Taiwan, it is the EUP that subducts beneath the PSP. The seismicity distribution, retrieved from the USGS catalogue, displays magnitude ranging from 2≤M≤7 between 1990 and 2019, shown in grey scale to indicate their depth and size, reflecting their magnitude. The solid red line with nothches denote the locations of the Manila and Ryukyu Trenches. Contour lines represent the depth of the plate interface at various levels, as indicated in the legend. The study area is marked by orange rectangles. **(b)** The geological regions in northern Taiwan are identified as follows: ECR (Eastern Central Range), BR (Backbone Range), HSR (Hsuehshan Range), WF (Western Foothills), CP (Coastal Plain), IP (Ilan Plain), TVG (Tatun Volcano Group), and the main faults, CF (Chuchih Fault) and LF (Lishan Fault). The seismicity used in this study is represented by colored circles, with magnitudes ranging from 3.7 ≤ M ≤ 5.8. The location of the Formosa Array (FM Array) seismic stations are indicated by black triangles, and the blue square symbols denote the locations of Broadband Array in Taiwan for Seismology (BATS) seismic stations.

The complicated tectonic setting of Taiwan can be discerned from the high seismic activity observed across most of its region. The island itself emerged above sea level due to the collision between the PSP and EUP. These collisions resulted in an active mountain range, including the ECR, BR, HSR, WF, and CP (Fig. 1b). The IP (Ilan Plain) represents the onshore extension of the Okinawa Trough, a back-arc basin associated with subduction at the Ryukyu Trench [13], while the TVG (Tatun Volcano Group) may be linked to the dehydration of the PSP oceanic crust.

3 Data and Method

3.1 Regional deep earthquake data

Table 1. List of events utilized in this study. DT (Date Time), LON (Longitude in geographical degree), LAT (Latitude in geographical degree), M (Magnitude) and Z (Depth in km)

No	DT	LON	LAT	M	Z
1	2019/03/12 04:19:15.15	121.86	25.02	5.3	138
2	2019/03/19 12:01:34.34	121.93	24.75	4.9	83.2
3	2019/03/22 20:05:48.48	122.45	24.49	4.9	88.8
4	2019/03/24 15:56:50.50	122.43	24.7	4.7	109.3
5	2019/04/01 10:54:35.35	122.24	24.93	5.1	128.6
6	2019/05/03 05:47:43.43	121.91	24.83	4.3	101.1
7	2019/05/08 23:48:47.47	122.49	24.82	5.1	122.7

The earthquake catalogue was obtained from the Central Weather Bureau (CWB) Taiwan for the years 2018 and 2019, encompassing magnitudes ranging from 3.7 to 5.8 and depths from 60 km to 140 km, located at the north - north eastern Taiwan. The corresponding seismograms were selected based on this catalog and cut to the event times using data from the Formosa Array (FM Array) datasets, which are managed by the Institute of Earth Sciences (IES) Academia Sinica and the Tatun Volcano Observatory (TVO). The FM Array is a dense seismic

network consisting of a total of 140 stations located in the northern part of Taiwan, with stations spaced approximately 5 kilometers apart. These seismic stations were originally established to investigate the geometry of the magma chamber beneath the Tatun Volcano Group (TVG), and serve other purposes such as hazard mitigation, particularly for the Taipei metropolitan area.

A total of 47 events met the specified criteria as shown in Fig. 1b (colored circle), and for this study we have utilized 7 of these events, as listed in Table 1.

3.2 Method

In this study, to identify the guided wave, we followed the procedure outlined by [3,10,14] to identify and calculate the body wave dispersion. This procedure is widely used to identify the guided phenomenon and to estimate the body wave dispersion curve in subduction zones worldwide.

To measure the high-frequency waves and their duration, we applied moving-window spectral analysis to obtain the ratio of high- to low-frequency signals (hp/lp ratio) from the *P*-wave arrival time to the 60 seconds of the dispersed signal. This procedure is clearly explained by [1]. The hp/lp ratio is determined by the following equation:

$$hp/lp\ ratio = A_{>3\,Hz}/A_{<2\,Hz} \quad (1)$$

The dominant frequency of the analyzed signal, calculated from the dispersion curve, was found to have an average of 3 Hz. Subsequently, a moving-window spectral analysis was applied using a high-pass filter with a 3 Hz and low-pass filter with a 2 Hz. The calculated spectrum from the moving-window spectral analysis was then applied to the Equation (1). In Equation (1), 'A' represents the median value of the Fourier spectrum amplitude.

4 Result and Discussion

4.1 Spectrogram of dispersed body wave

The spectrogram of dispersed signal is shown in Fig. 2. The characteristic of the dispersed body wave is demonstrated by the low-frequency signal arriving first at the *P*-wave onset, followed by the high-frequency signal.

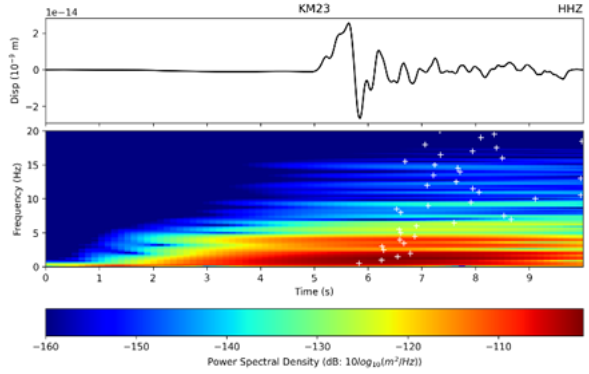

Fig. 2. Seismogram of HHZ component (top) and its spectrogram (bottom) of Event No. 1, as listed in Table 1, recorded by the KM23 FM Array seismic station. The '+' white symbol on the spectrogram indicates the maximum envelop corresponding to the frequency on the y-axis.

The finding of the spectrogram characteristics in this study are in agreement with the findings of the spectrogram of dispersed body wave signals in other subduction regions.

4.2 High-frequency seismic wave and its duration

The original signal of dispersed signal (event No. 1 listed in Table 1 as it is also shown in Fig. 2) is shown in Fig. 3 Top, the moving window of Hp 3 Hz is shown in Fig. 3 Center, and Fig. 3 Bottom is shown for Lp 2 Hz.

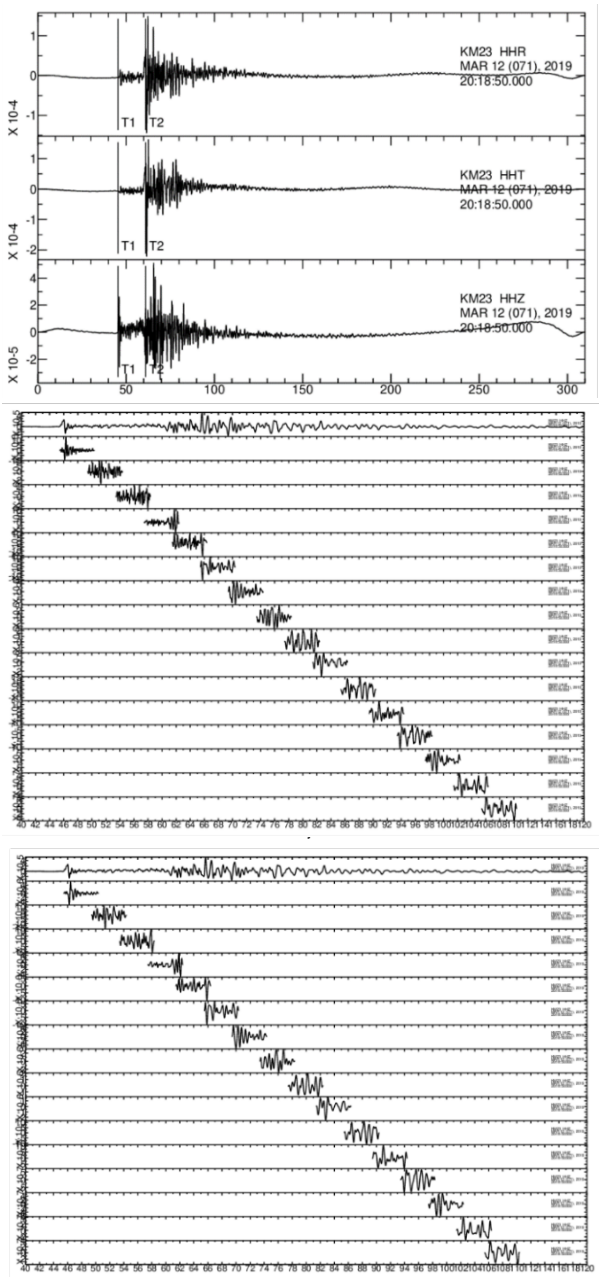

Fig. 3. Top: The original signal of event No. 1, as listed in Table 1, identified with guided wave characteristics, as indicated by the dispersed body wave signal in Fig. 2. This

signal was recorded by the KM23 station on its Radial (HHR), Transverse (HHT), and Horizontal (HHZ) components. **Center:** The filtered Hp 3 Hz of the original signal is shown in its entirety, covering the event duration of approximately 60 seconds after the *P*-wave arrival time onset. The moving window analysis is presented as a sequence of signals, each lasting 5 seconds and advancing in 4-seconds increments. **Bottom:** Similar to the center, but for the Lp 2 Hz.

When using the moving window spectral analysis, the duration is only considered if the ratio between Hp and Lp is higher than 1. Fig. 4 illustrates the calculated duration of Event No. 4, as listed in Table 1.

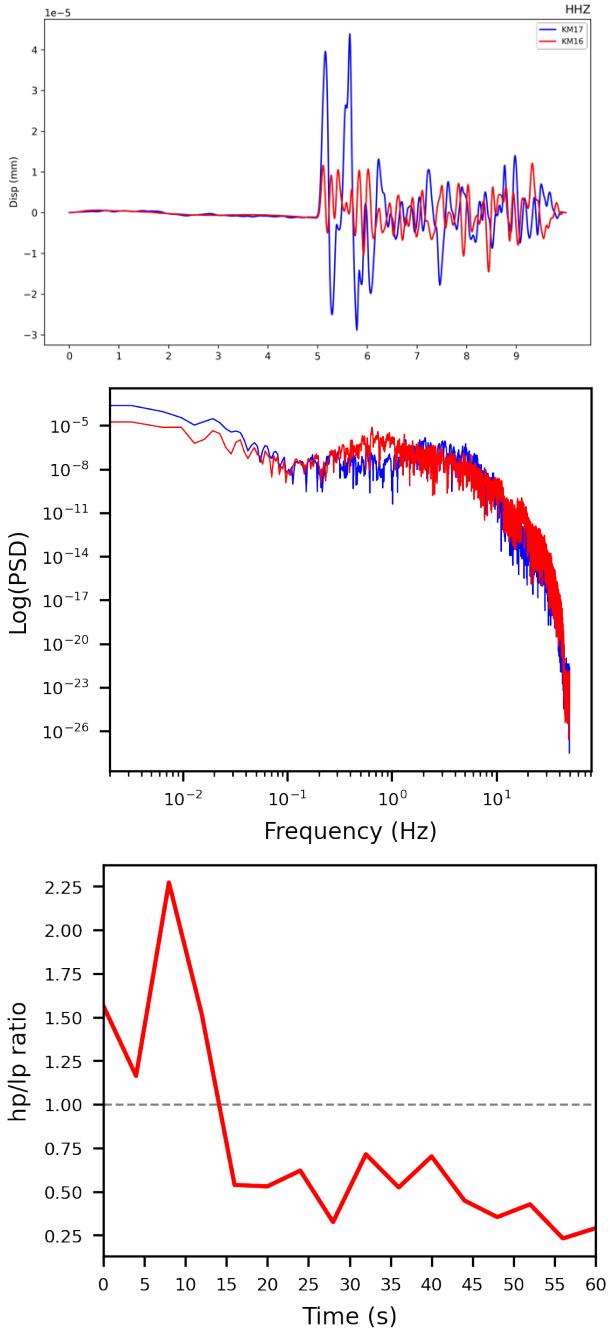

Fig. 4. Top: A comparison of the HHZ component seismogram between KM17 (observed guided wave) and KM 16 (not observed guided wave). **Center:** The amplitude spectrum of the signal, and **Bottom:** The Hp/Lp ratio with a dashed line at a ratio value of 1 is shown. The duration is only calculated for value above the dashed line; in this case, it is 14 seconds.

In Fig. 4, it is worth noting that the guided signal exhibits a significant amplitude at specific stations but not at others. Its overall spectrum indicates a higher amplitude at higher frequencies. Importantly the duration of the high-frequency wave is as long as 14 seconds.

4.3 Spatial distribution of high-frequency seismic wave

As the high-frequency wave and its duration vary among station for each event, it is observed that some stations had longer high-frequency waves, while others moderately observed the duration, and some even did not observed the guided phenomenon at all.

Fig. 5 is shown the spatial distribution of the high-frequency wave recorded by the stations during Event No. 4, as listed in Table 1.

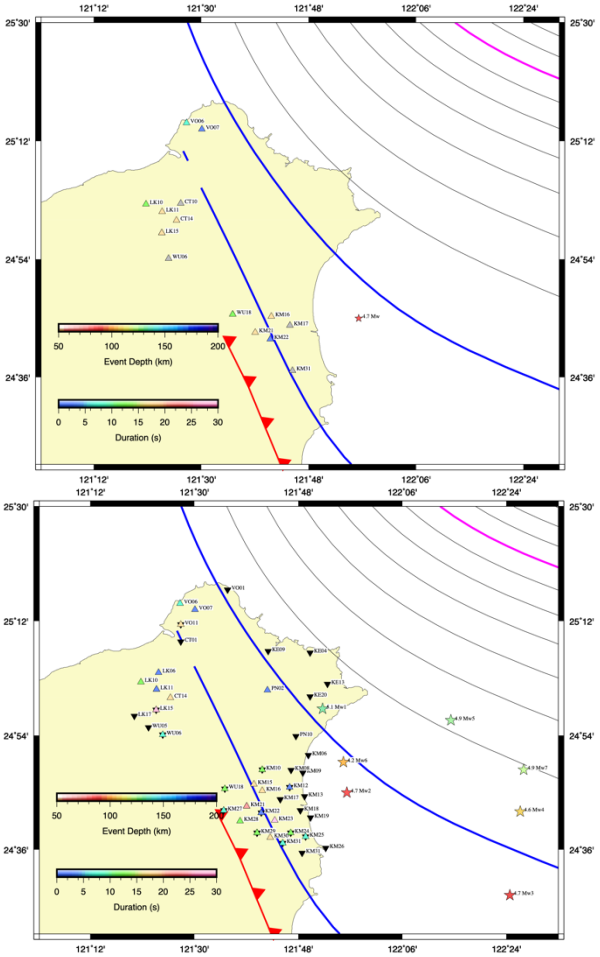

Fig. 5. Top: The spatial distribution of the observed guided wave during Event No. 4, as listed in Table 1 (star symbol), on the FM Array stations. The triangle symbols indicate the stations that observed the guided wave. The color on each triangle indicates the duration of the high-frequency waves, corresponding to the scalebar duration on the lower left. **Bottom:** Station that observed guided wave across all event used in this study (star symbols). The inverted triangles represent stations that have a dominant low-frequency wave.

It is evident that the guided phenomenon of the deep earthquake signal was not observed throughout all the FM Array stations. It appears that only specific stations, especially those situated at distances of 10 to 20 km

from the subduction interface, exhibits the guiding effect, and have a dominant high-frequency wave with an anomalous duration. The longest duration of high-frequency waves observed was as long as 35 seconds, as seen at stations KM 23, KM 21, and LK 15.

4.4 Discussion

The guided wave, as a result of slab-induced anomalous high-frequency waves with large amplitude from intermediate-depth earthquakes, highlights the importance of hazard assessment for these earthquakes [1,6,7]. The observations made in this study could also occur elsewhere in other subduction zones worldwide and may pose a greater threat if the corresponding region does not consider this effect as one of the hazards that may increase the disaster risk.

High-frequency waves, often termed "destructive waves" for residential buildings with 1 to 4 floors [15], are significantly influenced by the amplification phenomenon. Given that the guiding phenomenon amplifies both the amplitude and duration of these high-frequency waves, it becomes crucial to factor in these aspects when developing the Ground Motion Prediction Equation (GMPE) to account for potential abnormal intensity levels. This approach will enhance earthquake mitigation efforts in the area.

The slab structure may play an important role in the guiding effect; however, the distribution of the stations, i.e., source-to-receiver geometry [7], the subducting slab geometry [4,5], and geological properties [3,10,14,16], may intensify or nullify the observation. It is noteworthy that in Fig. 5 (bottom), the FM Array stations that situated along the northern part of HSR (Hsueshan Range) did not record any guiding phenomenon, possibly due to these issues, such as observed by [2] at the Manila Trench.

Besides its important in hazard mitigation, by identifying and measuring guided waves in subduction zones, it is possible to improve the modelling of various properties of the slab, including its shape, thickness, speed gradient, and variations in composition [1,2,5,7,17,18].

5 Conclusion

Intermediate to deep earthquakes within subduction zones often exhibit a guided wave phenomenon, resulting in the generation of high-amplitude, high-frequency waves. The observation of this phenomenon is notably influenced by factors like receiver-source geometry, slab geometry, and geological properties.

These heightened signals, arising from the guiding effect, have the potential to extend the duration of high-frequency waves, possibly leading to disastrous consequences. The prevalence of the guiding effect is most notable at seismic stations located within distances of 10 to 20 km from the subduction interface, displaying variable durations, with the longest recorded duration in this study being 35 seconds.

Hence, it becomes imperative to account for these considerations when formulating the GMPE to address potential deviations in intensity levels. In addition to its significance in hazard mitigation, the identification and measurement of guided waves within subduction zones offer opportunities to refine models of various slab properties, including its dimensions, thickness, speed gradients, and compositional variations.

Acknowledgements: We wish to extend our sincere appreciation to the Institute of Earth Sciences Academia Sinica (IES) and the Tatun Volcano Observatory (TVO), Taiwan, for granting us access to the FM Array dataset. The FM Array dataset is available upon request to IES and TVO. This study was supported by the Ministry of Education, Culture, Sciences, and Technology of the Republic of Indonesia, specifically through the Institute of Research and Community Service (LPPM) of Universitas Syiah Kuala as part of the Penugasan Penelitian Pusat Riset Katagori B scheme awarded to the Research Center for Marine Sciences and Fisheries, Universitas Syiah Kuala. The GMT software package was used to draw map figures [19].

References

1. K. H. Chen, B. L. N. Kennett, and T. Furumura, J. Geophys. Res. Solid Earth **118**, 665 (2013)
2. C. H. Lin, B. S. Huang, and R. J. Rau, Earth Planet. Sci. Lett. **174**, 231 (1999)
3. G. A. Abers and G. Sarker, Geophys. Res. Lett. **23**, 1171 (1996)
4. S. Martin and A. Rietbrock, Geophys. J. Int. **167**, 693 (2006)
5. T. Garth and A. Rietbrock, Earth Planet. Sci. Lett. **474**, 237 (2017)
6. B. L. N. Kennett and T. Furumura, Geophys. J. Int. **172**, 363 (2008)
7. T. Furumura and B. L. N. Kennett, J. Geophys. Res. Solid Earth **110**, 1 (2005)
8. H. A. Haridhi, B.-S. Huang, D. Sianipar, S. Purnawan, and I. Setiawan, E3S Web Conf. **339**, 02012 (2022)
9. H. A. Haridhi and D. Sianipar, IOP Conf. Ser. Earth Environ. Sci. **674**, (2021)
10. G. A. Abers, Earth Planet. Sci. Lett. **176**, 323 (2000)
11. H. Kanamori, W. H. K. Lee, and K. F. Ma, Geophys. J. Int. **191**, 126 (2012)
12. Y.-B. Tsai, Tectonophysics **125**, 17 (1986)
13. J. Lin, S. Hsu, A. T. Lin, Y. Yeh, and C. Lo, Tectonophysics **692**, **Part**, 181 (2016)
14. G. A. Abers, Phys. Earth Planet. Inter. **149**, 7 (2005)
15. H. Kanamori, L. Ye, B. S. Huang, H. H. Huang, S. J. Lee, W. T. Liang, Y. Y. Lin, K. F. Ma, Y. M. Wu, and T. Y. Yeh, Terr. Atmos. Ocean. Sci. **28**, 637 (2017)
16. M. E. Mann and G. A. Abers, Seismol. Res. Lett. **91**, 85 (2019)
17. B. R. Hacker, G. A. Abers, and S. M. Peacock, J. Geophys. Res. **108**, 2029 (2003)
18. B. R. Hacker, S. M. Peacock, G. A. Abers, and

S. D. Holloway, J. Geophys. Res. Solid Earth **108**, 2030 (2003)

19. P. Wessel and W. H. F. Smith, Eos, Trans. Am. Geophys. Union **79**, 579 (1998)